Inductance in One-Dimensional Nanostructures

Toshishige Yamada, *Member, IEEE*, Francisco R. Madriz, and Cary Y. Yang, *Fellow, IEEE*

(Invited Paper)

***Abstract*—The physical origin of kinetic inductance is examined for 1-D nanostructures, where the Fermi liquid theory prevails. In order to have appreciable kinetic inductance, ballistic transport must exist, with no inelastic scattering inside the nanowires. Kinetic inductance is assigned to the nanowire itself and independent of its surroundings, whereas magnetic inductance is assigned to the nanowire and substrate. Kinetic and magnetic inductances are in series in an equivalent circuit representation. If there are m transmission modes and n multiwalls in the nanostructure, kinetic inductance decreases by a factor of $1/(mn)$. The relation of the predicted results to preliminary experimental findings is discussed.**

***Index Terms*—Ballistic transport, Fermi liquid, kinetic inductance, 1-D nanostructures.**

I. Introduction

KINETIC inductance, which is well known in superconductors [1], [2], has been gathering significant attention in studies of nanodevices and circuits [3]–[8]. There are numerous reports on it, but many concentrate on the system-level study, i.e., how nanowire network characteristics are modified with kinetic inductance. Here, we examine its physical origin and significance in device/circuit applications. Multiwall 1-D nanostructures with multiple transmission modes are considered. While carbon nanotubes are used as examples, results here can be applied to any 1-D multiwall nanostructures.

The relation between the Coulomb energy q^2/C' and a quantity E_F/λ in the nanowire determines the nature of transport [9], where q is the unit electronic charge, C' is the nanowire capacitance per unit length, E_F is the Fermi level, and λ is the 1-D electron density. When $q^2/C' \ll E_F/\lambda$, the Fermi liquid theory (independent electron picture) prevails [10]–[12], and when $q^2/C' \sim E_F/\lambda$, the Tomonaga–Luttinger theory (strongly correlated electron picture) prevails [13], [14]. We will concentrate on the situations where the Fermi liquid theory prevails. Then, current is carried by individual electrons (quasiparticles) with spin 1/2 as in bulk semiconductors, and the signal is transmitted with a speed of Fermi velocity v_F.

Fig. 1 shows situations for the nanowire and substrate through which constant current I flows. The system stores static magnetic energy and electrostatic energy and also dissipates power. The stored and dissipated energies are related to inductance L, capacitance C, and resistance R, respectively. The problem is how we classify the total electron kinetic energy E_k. If transport is scattering based (ohmic) [15], as shown in Fig. 1(a), then electron kinetic energy will be converted to Joule's heat after inelastic collision with the background lattice. Thus, E_k can be incorporated into R. However, if transport is ballistic [16]–[19], as shown in Fig. 1(b), there is no Joule heating *inside* the nanowire. In this case, resistance is considered to arise at electrode contacts, where electrons move between a macroscopic electrode with an infinite number of modes and a nanowire with a small number of modes. Electron energy relaxation is considered to occur *outside* the nanowire, i.e., in electrodes. Joule heating is absent *inside* the nanowire, and it is inappropriate to incorporate E_k into R. Since average electron velocity is related to current I, it is quite natural to incorporate it into L. This is the origin of kinetic inductance L_k, and it is defined by $(1/2)L_kI^2 = E_k$.

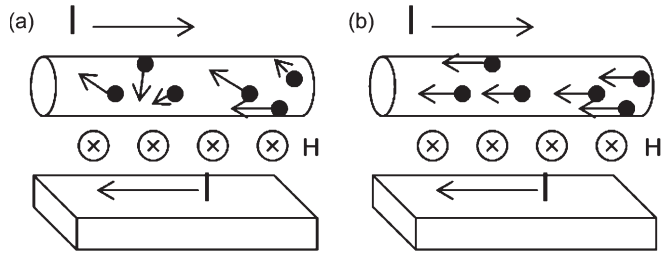

Fig. 1. Nanowire and substrate with current I, where dots represent electrons and H represents magnetic field. (a) Classical transport with many inelastic scattering events. (b) Ballistic transport with practically no scattering events.

In studying inductance in nanowires, the following scenarios are examined: (i) L_k coexists with a magnetic inductance L_m, as illustrated in Fig. 1(b). The magnetic inductance is defined by $L_m = \Phi/I$, where Φ is the magnetic flux penetrating through the plane of the nanowire and substrate. The total energy $E_{\rm sys}$ added to the system per unit length during Δt to maintain the current I is expressed by the sum of dissipated energy, stored magnetic energy, and stored electrostatic energy, i.e.,

$$E_{\rm sys} = \int_0^{\Delta t} I^2 R\, dt + \frac{1}{2}LI^2 + \frac{1}{2}CV^2. \tag{1}$$

The first term in $E_{\rm sys}$ is due to Joule heating at the electrodes. Thus, the energy $E_{\rm nw}$ stored *inside* the ballistic nanowire is

$$E_{\rm nw} = \frac{1}{2}LI^2 + \frac{1}{2}CV^2. \tag{2}$$

Manuscript received February 18, 2009; revised June 15, 2009. Current version published August 21, 2009. This work was supported by the U.S. Army Space and Missile Defense Command SMDC and carries Distribution Statement A, approved for public release, distribution unlimited. The review of this paper was arranged by Editor S. Saha.

The authors are with the Center for Nanostructures, Santa Clara University, Santa Clara, CA 95053 USA (e-mail: tyamada@scu.edu).

Digital Object Identifier 10.1109/TED.2009.2026202

The first term in $E_{\rm nw}$ represents the sum of magnetic energy and kinetic energy E_k. Thus, $L = L_m + L_k$, or L_m and L_k must be in series in an equivalent circuit representation. (ii) L_k does not exist if transport is ohmic with many inelastic scattering events, as illustrated in Fig. 1(a). The nanowire resistance is proportional to its length, and E_k must be incorporated into nanowire R, and it is redundant to discuss L_k. (iii) While scenarios (i) and (ii) can be considered mutually exclusive, this scenario provides a unified description of inductance in nanowires. L_m is assigned to the nanowire–substrate system. Thus, the same nanowire can have different L_m depending on its surroundings, whereas L_k is assigned to the nanowire itself along the wire direction as it represents electron kinetic energy gain during its ballistic transport.

II. Kinetic Inductance in Single-Wall 1-D Nanostructures

If transport is ballistic, the system resistance $R_{\rm sys}$ between two electrodes is given by the Landauer–Bütticker formalism [16]–[18]. In a nanowire, the current ΔI for applied voltage ΔV is expressed by

$$\Delta I = q v_F \Delta N = q v_F [n_F q \Delta V]. \tag{3}$$

ΔN represents the number of electrons per unit length contributing to transport because of bias ΔV. v_F is the electron Fermi velocity, and n_F is the 1-D electronic state density at the Fermi level E_F given by the E–k relation. They are

$$v_F = \frac{1}{\hbar}\frac{dE}{dk}\bigg|_{E=E_F} \tag{4}$$

$$n_F = \frac{2}{2\pi}\frac{dk}{dE}\bigg|_{E=E_F} = \frac{2}{2\pi}\frac{1}{\hbar v_F}. \tag{5}$$

Here, $\hbar$ is the reduced Planck's constant. Thus, the $v_F n_F$ product is a constant $1/\pi\hbar$, regardless of the E–k relation. It should be noted that this relation holds only in 1-D systems, as is obvious from (5). In fact, in 2-D and 3-D systems, n_F is proportional to kdk/dE and $k^2 dk/dE$ and $v_F n_F$ depends on k and k^2, respectively. Considering the spin degeneracy of 2, the quantum conductance G_Q is defined by

$$\Delta I = \frac{2q^2}{2\pi\hbar}\Delta V \equiv G_Q \Delta V. \tag{6}$$

The existence of such ballistic transport was experimentally confirmed for a single-wall carbon nanotube by extracting this G_Q value ($G_Q^{-1} = 12.9$ kΩ) [19]. It must be emphasized that this observation was made for a micrometer-long nanotube at room temperature, which is the usual measurement condition.

Now, kinetic energy is increased by $\Delta^2 E_k$ per unit length due to ΔV compared to that in thermal equilibrium. Inside the nanowire, the potential energy $q\Delta V$ at the source with respect to the drain will fully be converted to kinetic energy in ballistic transport. On average, the excess electron kinetic energy is

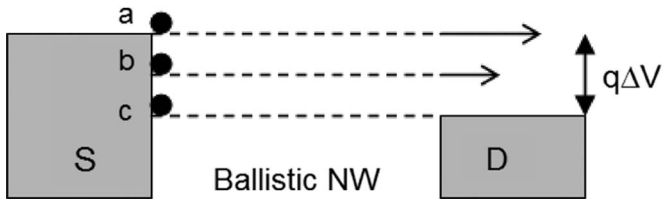

Fig. 2. Energy band diagram for the system "source electrode biased at 0—ballistic nanowire—drain electrode biased at $\Delta V > 0$." Three electrons a, b, and c will ballistically run through the wire. At the drain edge, they gain kinetic energy of $q\Delta V$, $q\Delta V/2$, and 0, respectively. Thus, the average kinetic energy gain is $q\Delta V/2$.

$q\Delta V/2$, and there are ΔN electrons per unit length, as shown in Fig. 2. Thus, using (5)

$$\Delta^2 E_k = \frac{q\Delta V}{2}\Delta N = \frac{q\Delta V}{2} n_F q \Delta V = \frac{q^2}{2\pi\hbar v_F}(\Delta V)^2. \tag{7}$$

It should be noted that the detailed E–k relation is not needed here. By using G_Q, we can express ΔV by $\Delta I/G_Q$, yielding

$$\begin{aligned}\Delta^2 E_k &= \frac{1}{2}\frac{q^2}{\pi\hbar v_F}\left(\frac{\Delta I}{G_Q}\right)^2 \\ &= \frac{1}{2}\frac{q^2}{\pi\hbar v_F G_Q^2}(\Delta I)^2 \equiv \frac{1}{2}L_k'(\Delta I)^2.\end{aligned} \tag{8}$$

Thus, kinetic inductance L_{k1}' per unit length per mode is given by

$$L_{k1}' = \frac{q^2}{\pi\hbar v_F G_Q^2} = \frac{\pi\hbar}{v_F q^2}. \tag{9}$$

If there are multiple transmission modes m in the nanowire, then n_F is replaced by mn_F, or $1/v_F$ is replaced by m/v_F in (7), but G_Q is also replaced by mG_Q in (8). Accordingly, $\Delta^2 E_k$ increases by a factor of m, and ΔI^2 increases by a factor of m^2. It should be noted that $\Delta I^2 \propto m^2$ does not mean $L_{km}' \propto m^2$ since kinetic energy increases by m. Thus

$$L_{km}' = \frac{q^2}{\pi\hbar v_F G_Q^2}\frac{1}{m} = \frac{\pi\hbar}{v_F q^2}\frac{1}{m} = \frac{L_{k1}'}{m}. \tag{10}$$

Kinetic inductances given by (9) and (10) are considered to be approximate. Depending on the detailed model used, final results may have different numerical factors. For example, the density of states with m modes has been assumed to be mn_F, but different values could be obtained by assuming a specific E–k relation.

By assuming $v_F \sim 8 \times 10^5$ m/s for a graphene sheet [9], we estimate that $L_{k1}' \sim 16$ nH/μm in the 1-D limit, where only one transmission mode participates in transport. As the number of modes m increases, kinetic inductance rapidly decreases as $1/m$. Because of this effect, kinetic inductance is significantly reduced. For a single-wall nanostructure with m modes, $L' = L_m' + L_{k1}'/m$.

III. Inductance in Multiwall 1-D Nanostructures

The inductance of a double-walled nanotube in Fig. 3(a) is first considered. In Section II, we have shown that magnetic

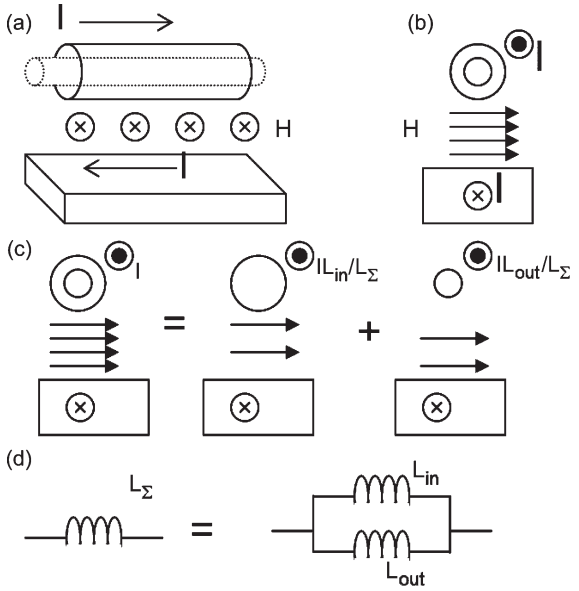

Fig. 3. (a) Multiwall nanotube and substrate supporting current I. (b) Side view showing the magnetic field. (c) Multiwall nanotube decomposed into two nanotubes, where the outer wall conducts $IL_{\rm in}/L_\Sigma$ and the inner wall conducts $IL_{\rm out}/L_\Sigma$. (d) Its equivalent circuit with parallel inductances $L_{\rm in}$ and $L_{\rm out}$.

and kinetic inductances are connected in series by $L' = L'_m + L'_{k1}/m$. Thus, how inductance depends on the number of walls is the same as traditional magnetic inductance cases. Let us assume that the inner and outer walls have $L'_{\rm in}$ and $L'_{\rm out}$, respectively. The magnetic field is created, as shown in Fig. 3(b), between the nanotube and substrate. When current I is applied, $IL'_{\rm in}/L_\Sigma$ flows in the outer wall, and $IL'_{\rm out}/L_\Sigma$ flows in the inner wall, where $L_\Sigma = L'_{\rm in} + L'_{\rm out}$. This can be justified by considering impedance elements of $j\omega L'_{\rm in}$ and $j\omega L'_{\rm out}$ and taking the dc limit. The same conclusion can be reached from free energy considerations. The magnetic energy U_m related to current I is

$$U_m = \frac{1}{2}L'_{\rm in}I^2_{\rm in} + \frac{1}{2}L'_{\rm out}I^2_{\rm out} \tag{11}$$

where $I = I_{\rm in} + I_{\rm out}$. For fixed I, U_m is minimized when the fluxes are the same, i.e., $L'_{\rm in}I_{\rm in} = L'_{\rm out}I_{\rm out}$. Therefore, $IL'_{\rm in}/L_\Sigma$ flows in the outer wall, and $IL'_{\rm out}/L_\Sigma$ flows in the inner wall, which is consistent with the aforementioned impedance argument. Thus, the situation in Fig. 3(b) can be decomposed into two independent inductance elements, as shown in Fig. 3(c), yielding an equivalent circuit, as given in Fig. 3(d).

L'_m for a cylinder–substrate system is evaluated and is given by [19]

$$L'_m = \frac{\mu}{2\pi}\ln\left[\frac{2h}{d} + \sqrt{\frac{4h^2}{d^2} - 1}\right] \approx \frac{\mu}{2\pi}\ln\left[\frac{4h}{d}\right] \tag{12}$$

where h is the distance between the nanotube center and the substrate, d is the nanotube diameter, and μ is the permeability. For $h = 10d$, $L'_m = 0.74$ pH/μm; for $h = 100d$, $L'_m = 1.2$ pH/μm; and even for $h = 1000d$, $L'_m = 1.7$ pH/μm. Thus, $L'_{k1} \sim 16$ nH/μm dominates L'_m in *ballistic* nanostructures, but if there are many transmission modes, magnetic inductance may not be negligible.

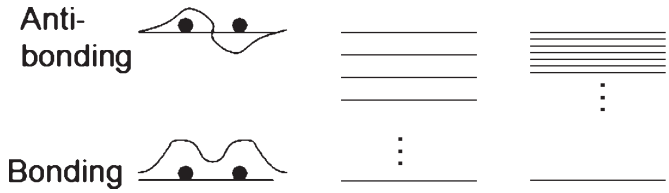

Fig. 4. Subband formation with bonding and antibonding states for a $(k, 0)$ zigzag nanotube. From left to right, subbands for a single-hexagon unit cell with bonding and antibonding levels (left, $k = 1$), a multiple-hexagon unit cell (middle, intermediate k), and many hexagon unit cells (right, large k) are shown, respectively. There are $2k$ subbands in the $(k, 0)$ nanotube. Regardless of the number of hexagons in the unit cell, the highest and lowest energy levels are almost the same.

Generally, if there are n walls in the nanotube, inductance is reduced by $1/n$ (assuming inductance values for different walls are the same). It is interesting to note that a single-wall nanotube with m different modes can be regarded as a multiwall nanotube with m walls having a single mode, assuming the magnetic inductance is negligible in either case. As a result, if a nanotube has n walls with m modes each, then

$$L' = \frac{L'_m + L'_{k1}/m}{n} \approx \left(\frac{0.001}{n} + \frac{16}{mn}\right) \qquad [\text{nH}/\mu\text{m}]. \tag{13}$$

We have used the tight-binding theory [21] and estimated m. A single-wall zigzag (10, 0) semiconducting carbon nanotube has a diameter of 0.783 nm [22]. This can be regarded as an extreme 1-D nanotube since the other subbands are separated from the Fermi level by 1.2 eV, which is about 50 times larger than the thermal energy at 300 K. The conduction and valence bandwidths are both 7.5 eV, and there are 20 states or subbands. This is because a carbon atom provides one state, i.e., one p-orbital, and there are two carbon atoms in the unit hexagon. A linear combination of these two p-orbitals forms two states, namely, bonding and antibonding states. A (10,0) nanotube has ten hexagons in a unit cell. The unit cell has 20 p-orbitals and therefore, there should be 20 subbands within the same bandwidth. In fact, the bandwidth is insensitive to the number of periods since the top and bottom of the band are related to antibonding and bonding states, whose energies are determined by the behavior of *two* carbon atoms in the hexagon cell [19]. This situation is depicted in Fig. 4. Thus, a single-wall zigzag (1000, 0) carbon nanotube with a diameter of 78.3 nm has 200 000 states within the same bandwidth.

According to the Fermi liquid theory, only electrons in the thermal energy window near E_F can participate in transport. A (1000, 0) nanotube has a diameter of 78.3 nm, and for the thermal energy window of 0.026 eV at 300 K, there would be $0.026/7.5 \times 200\,000 = 693$ states participating in transport. A single-wall zigzag (2000, 0) nanotube has a diameter of 157 nm, and for the same thermal energy window, there would be 1386 states. Thus, $m = 693$ for a (1000, 0) nanotube with a diameter of 78.3 nm, and $m = 1386$ for a (2000, 0) nanotube with a diameter of 157 nm. Accordingly, a 100-nm-diameter nanotube has $m = 884$, and a 150-nm-diameter nanotube has $m = 1324$. Therefore, a 100-nm-diameter single-wall nanotube has $L' \sim$ (magnetic) 1 pH/μm + (kinetic) 18 pH/μm. A 150-nm-diameter single-wall nanotube has $L' \sim$ (magnetic)

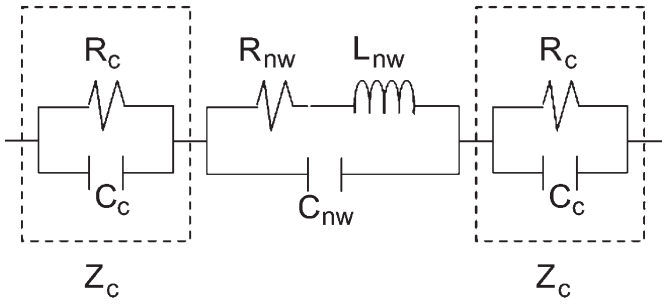

Fig. 5. Equivalent circuit to extract $L_{\rm nw}$, which is used in [6] for their ac analysis. In [4], $C_{\rm nw}$ is absent from the beginning. Enclosed regions with dashed lines represent the CNF–electrode contacts.

1 pH/μm + (kinetic) 12 pH/μm. These values must be divided by n when the nanotube is multiwalled. For $n \sim 100$, a 100-nm-diameter nanotube has $L' \sim$ (magnetic) 0.01 pH/μm + (kinetic) 0.18 pH/μm, and a 150-nm-diameter nanotube has $L' \sim$ (magnetic) 0.01 pH/μm + (kinetic) 0.12 pH/μm, respectively. In nanotubes with ohmic transport, kinetic inductance is absent, and only the first term contributes to L'.

IV. Possible Measurement Scheme

We have previously designed and fabricated a test structure to study the high-frequency characteristics of 1-D nanostructures and have reported results for carbon nanofibers (CNFs) [23]. Using the same test structure, it is possible to examine the extent to which inductance affects the measured S-parameters for any 1-D systems. Adopting a similar parameter extraction scheme as in [23], we find that the ground–signal–ground *open* test structure (with CNF absent) contains an inductive component in the signal pads, which is determined to be 1.0 pH/μm. This value turns out to have a negligible effect on the transmission parameter $S_{21}(\omega)$ in the presence of CNF. With CNF in contact with gold electrodes in the test structure, $S_{11}(\omega)$ and $S_{21}(\omega)$ are measured from 1 to 50 GHz for a 1-μm-long CNF with a 150-nm diameter. From these measured S-parameters, an impedance for the test device can be extracted.

From the extracted impedance, it would then be possible to study the behavior using a circuit model such as the model proposed in [6] and shown in Fig. 5, where all circuit elements can be frequency dependent. The presence of C_c can easily be understood since the CNF–electrode contact can be treated as a capacitor. Unlike other treatments [4], which remove $C_{\rm nw}$ at the outset of the analysis, the equivalent circuit in Fig. 5 is the most complete lumped-parameter description of a 1-D nanostructure. At low frequencies, $L_{\rm nw}$ is a virtual short, and the circuit is capacitive. At higher frequencies, where $R_{\rm nw}$ and $\omega L_{\rm nw}$ are comparable, $L_{\rm nw}$ is becoming observable. At very high frequencies, well above the resonant frequency $\omega_{\rm res} = [(C_{\rm nw} + C_c/2)L_{\rm nw}]^{-1/2}$, $L_{\rm nw}$ is practically open, and the circuit is again capacitive, but $\omega_{\rm res}$ is typically on the order of terahertz, which is much higher than our measurement frequencies.

Based on the circuit model in Fig. 5, R_c and $R_{\rm nw}$ are determined to be about 5 kΩ, and C_c and $C_{\rm nw}$ are determined to be about 0.1 fF. It is also determined that $L'_{\rm nw}$, which includes both magnetic and kinetic inductances, has to satisfy $0 < L'_{\rm nw} < \sim 0.1$ nH/μm to reproduce measured $S_{21}(\omega)$ data. This suggests that $L_{\rm nw}$ does not play a critical role, since in this inductance range, the relation $R_{\rm nw} \gg \omega L_{\rm nw}$ is easily satisfied up to 50 GHz. Since our CNFs exhibit ohmic transport [24] and kinetic inductance is absent, we estimate $L'_{\rm nw} \sim L'_m \sim 1/n$ pH/μm according to (13). CNFs have a stacked-cup structure in the interior, surrounded by cylindrical graphene walls [24]. The number of walls n in the CNFs studied ranges between 10 and 100, so that $L'_{\rm nw} \sim 0.01-0.1$ pH/μm. Our estimation of $0 < L'_{\rm nw} < \sim 0.1$ nH/μm from experiments is consistent with this theoretical prediction, but the upper limit from experiments is still orders of magnitude larger than the predicted value.

For more accurate extraction of inductance, $R_{\rm nw} \sim \omega L_{\rm nw}$ must be satisfied so that $\omega L_{\rm nw}$ can have a measurable effect in the equivalent circuit. This means reducing $R_{\rm nw}$ by improving the CNF quality so that near-ballistic transport is achieved and kinetic inductance is present, and/or increasing measurement frequency beyond 50 GHz. In fact, in the ballistic limit, a 1-μm single-wall $(n = 1)$ nanotube with a very small diameter so that only one mode $(m = 1)$ is relevant to transport, $R_{\rm nw} \sim 0$, $R_c \sim h/2q^2 = 12.9$ kΩ, and $L_k \sim 16$ nH. Magnetic inductance is negligibly small, and kinetic inductance observation at frequencies above 100 GHz might be possible. Similarly, a 1-μm multiwall nanotube with a very small diameter $(m = 1)$ yields $R_{\rm nw} \sim 0$, $R_c \sim 12.9/n$ kΩ, and $L_k \sim 16/n$ nH. Thus, kinetic inductance observation might also be possible. However, a CNT with a large diameter has many modes $(m \gg 1)$, and from (13), L_k becomes negligible compared with L_m. Then, kinetic inductance extraction might not be easy in this case.

Differentiation between magnetic and kinetic inductances is a challenging task, as they are simultaneously present in nanostructures. Generally, the measured inductance value represents both contributions, but inductance measurement as a function of temperature T might be one way to distinguish between them. Magnetic inductance is determined by how the magnetic field is created in the system and has nothing to do with transport inside the nanotube for a given current through it. Thus, it is largely independent of T. However, kinetic inductance requires ballistic transport, as discussed in Section I. Generally, if T is higher, there is more phonon scattering, and transport in a given material tends to be ohmic. Accordingly, kinetic inductance would be present at low T but would disappear at high T. At low T, both magnetic and kinetic inductances contribute, but at high T, only magnetic inductance contributes, and based on this, it would be possible to experimentally extract both values.

For high-frequency applications, emphasis will be on near-ballistic nanotubes. Using a multiwall nanotube or an array of single-wall nanotubes would allow one to vary the inductance value using (13) according to the frequency range of interest. CNF reliability is another important issue in interconnect applications. We have studied the breakdown of CNFs due to Joule heating and found that the maximum current density is well above 10^6 A/cm^2 and is critically dependent on the CNF length and how the CNF is contacted to the substrate and electrodes [25]–[27]. The maximum current density is not a material

constant, but it is determined by how the heat is dissipated in the system. It is expected that all carbon nanostructures consisting of C–C covalent bonds are more resistant to electromigration than conventional metals. Additional consideration of ohmic versus ballistic transport in the context of length dependence [15], [28] will be the subject of future studies.

V. Conclusion

We have examined the origin of kinetic inductance in 1-D nanostructures, where the Fermi liquid theory applies, and have estimated kinetic inductance for a nanotube with m modes and n walls. Nanowires must support ballistic transport to have appreciable kinetic inductance. There is no kinetic inductance if transport is ohmic. The estimated combined kinetic and magnetic inductances are compared with preliminary experimental findings based on results of S-parameter measurements on CNFs.

Acknowledgment

The authors would like to thank T. Saito, J. Jameson, and N. Akhavantafti for useful discussions.

References

[1] R. Meservey and P. M. Tedrow, "Measurements of the kinetic inductance of superconducting linear structures," *J. Appl. Phys.*, vol. 40, no. 5, pp. 2028–2034, Apr. 1969.
[2] D. M. Sheen, S. M. Ali, D. E. Oates, R. S. Withers, and J. A. Kong, "Current distribution, resistance, and inductance for superconducting strip lines," *IEEE Trans. Appl. Supercond.*, vol. 1, no. 2, pp. 108–115, Jun. 1991.
[3] P. J. Burke, "Luttinger liquid theory as a model of the gigahertz electrical properties of carbon nanotubes," *IEEE Trans. Nanotechnol.*, vol. 1, no. 3, pp. 129–144, Sep. 2002.
[4] J. J. Plombon, K. P. O'Brien, F. Gstrein, V. M. Dubin, and Y. Jiao, "High-frequency transport electrical properties of individual and bundled carbon nanotubes," *Appl. Phys. Lett.*, vol. 90, no. 6, p. 063 106, Feb. 2007.
[5] M. Zhang, X. Huo, P. C. H. Chan, Q. Liang, and Z. K. Tang, "Radio-frequency transmission properties of carbon nanotubes in a field-effect transistor configuration," *IEEE Electron Device Lett.*, vol. 27, no. 8, pp. 668–670, Aug. 2006.
[6] S. C. Jun, X. M. Huang, S. W. Moon, H. J. Kim, J. Hone, Y. W. Jin, and J. M. Kim, "Passive electrical properties of multi-walled carbon nanotubes up to 0.1 THz," *New J. Phys.*, vol. 9, no. 8, p. 265 (1-10), 2007.
[7] G. F. Close and H.-S. P. Wong, "Fabrication and characterization of carbon nanotube interconnects," in *IEDM Tech. Dig.*, 2007, pp. 203–206.
[8] H. Li and K. Banerjee, "High frequency effects in carbon nanotube interconnects and implication for on-chip inducer design," in *IEDM Tech. Dig.*, 2008, pp. 525–528.
[9] R. Tarkiainen, M. Ahlskog, J. Penttila, L. Roschier, P. Hakonen, M. Paalanen, and E. Sonin, "Multiwalled carbon nanotube: Luttinger versus Fermi liquid," *Phys. Rev. B, Condens. Matter*, vol. 64, no. 19, p. 195 412, Nov. 2001.
[10] L. D. Landau, "The theory of a Fermi liquid," *Sov. Phys. JETP*, vol. 3, pp. 920–925, 1957.
[11] L. D. Landau, "Oscillations in a Fermi liquid," *Sov. Phys. JETP.*, vol. 5, pp. 101–108, 1957.
[12] L. D. Landau, "On the theory of a Fermi liquid," *Sov. Phys. JETP.*, vol. 8, pp. 70–74, 1958.
[13] S. Tomonaga, "Remarks on Bloch's method of sound waves applied to many-Fermion problems," *Prog. Theor. Phys.*, vol. 5, no. 4, pp. 544–569, 1950.
[14] J. M. Luttinger, "An exactly solvable model of a many-Fermion system," *J. Math. Phys.*, vol. 4, no. 9, pp. 1154–1162, Sep. 1963.
[15] C. W. J. Beenakker and H. van Houten, *Solid State Physics*, vol. 44, H. Ehrenreich and D. Turnbull, Eds. New York: Academic, 1991.
[16] R. Landauer, "Electrical resistance of disordered one-dimensional lattice," *Philos. Mag.*, vol. 21, no. 172, pp. 863–867, Apr. 1970.
[17] Y. Imry, "Physics of mesoscopic systems," in *Directions in Condensed Matter Physics*, G. Grinstein and G. Mazenko, Eds. Singapore: World Scientific, 1986, pp. 101–163.
[18] M. Bütticker, "Symmetry of electrical conduction," *IBM J. Res. Develop.*, vol. 32, no. 3, pp. 317–334, May 1988.
[19] S. Frank, P. Poncharal, Z. L. Wang, and W. A. de Heer, "Carbon nanotube quantum resistors," *Science*, vol. 280, no. 5370, pp. 1744–1746, Jun. 1998.
[20] F. T. Ulaby, *Fundamentals of Applied Electromagnetics*. Englewood Cliffs, NJ: Prentice–Hall, 1997.
[21] W. A. Harrison, *Electronic Structure and the Properties of Solids*. New York: Dover, 1989.
[22] M. S. Dresselhaus, G. Dresselhaus, and P. C. Eklund, *Science of Fullerenes and Carbon Nanotubes*. San Diego, CA: Academic, 1997.
[23] F. R. Madriz, J. R. Jameson, S. Krishnan, X. Sun, and C. Y. Yang, "Circuit modeling of high-frequency conduction in carbon nanofibers," *IEEE Trans. Electron Devices*, vol. 56, no. 8, pp. 1557–1561, Aug. 2009.
[24] Q. Ngo, T. Yamada, M. Suzuki, Y. Ominami, A. M. Cassell, J. Li, M. Meyyappan, and C. Y. Yang, "Structural and electrical characterization of carbon nanofibers for interconnect via applications," *IEEE Trans. Nanotechnol.*, vol. 6, no. 6, pp. 688–695, Nov. 2007.
[25] H. Kitsuki, T. Yamada, D. Fabris, J. R. Jameson, P. Wilhite, M. Suzuki, and C. Y. Yang, "Length dependence of current-induced breakdown of carbon nanofibers," *Appl. Phys. Lett.*, vol. 92, no. 17, p. 173 110, May 2008.
[26] T. Saito, T. Yamada, D. Fabris, H. Kitsuki, P. Wilhite, M. Suzuki, and C. Y. Yang, "Improved contact for thermal and electrical transport in carbon nanofiber interconnects," *Appl. Phys. Lett.*, vol. 93, no. 10, p. 102 108, Sep. 2008.
[27] T. Yamada, T. Saito, D. Fabris, and C. Y. Yang, "Electrothermal analysis of breakdown in carbon nanofiber interconnects," *IEEE Electron Device Lett.*, vol. 30, no. 5, pp. 469–471, May 2009.
[28] A. N. Andriotis, M. Menon, and L. Chernozatonskii, "Nonlinear resistance dependence on length in single-wall carbon nanotubes," *Nano Lett.*, vol. 3, no. 2, pp. 131–134, Feb. 2003.

Toshishige Yamada (M'93) received the B.S. and M.S. degrees in physics from the University of Tokyo, Tokyo, Japan, and the Ph.D. degree in electrical engineering from Arizona State University, Tempe, under the supervision of Prof. D. K. Ferry.

He is currently Research Professor of Engineering at Santa Clara University, Santa Clara, CA. He worked for NEC Microelectronics Research Laboratories, Japan, and NASA Ames Research Center. He has conducted physical modeling/analysis of nano/micromaterials and devices such as the Josephson latch device, quantum wire, lateral surface superlattice, strained-Si channel on SiGe substrate, atomic chain on substrate, nanotube FET, nanotube–STM system, gated nanotube semiconductor–metal diode, nanotube gas sensor and Schottky barrier (oxygen, ammonia), nanofiber device, nanowire FET (indium oxide, zinc oxide), nanowire device (indium antimonide), and metallic nanoisland (lead on silicon), emphasizing comparison with experiments. He is currently extending his activities to the study of thermal and electrical properties of carbon nanostructures.

Prof. Yamada is a member of Phi Kappa Phi and Sigma Xi. He currently serves on the Editorial Board of *Journal of Computational and Theoretical Nanoscience* and on the Committee of IEEE Santa Clara Valley Electron Device Society.

Francisco R. Madriz was born in Managua, Nicaragua. He received the B.S. degree in electrical engineering from the University of California, Davis, in 1995 and the M.S. degree in electrical engineering from San Jose State University, San Jose, CA, in 2000. He is currently working toward the Ph.D. degree in electrical engineering at Santa Clara University, Santa Clara, CA. His doctoral thesis consists in the RF/microwave circuit modeling of high-frequency 1-D electrical conduction in carbon-based nanodevices.

His main areas of interests include the design of passive and active microwave circuits and high-frequency circuit modeling of carbon-based nanodevices.

Cary Y. Yang (F'99) received the B.S., M.S., and Ph.D. degrees from the University of Pennsylvania, Philadelphia, in 1970, 1971, and 1975, respectively, all in electrical engineering.

In 1976, he joined Massachusetts Institute of Technology, Cambridge, as a Postdoctoral Fellow, working on the detailed electronic structure of chemisorbed molecules on heavy transition metal surfaces. He continued his research on surface and interface science at NASA Ames Research Center and Stanford, before founding Surface Analytic Research, a Silicon Valley company focusing on sponsored research projects covering various applications of surfaces and nanostructures. In 1983, he joined Santa Clara University, Santa Clara, CA where he is currently Professor and Chair of Electrical Engineering and Director of Center for Nanostructures. His research is on nanostructure interfaces and interconnects in electronic and biological systems.

Prof. Yang was an Editor of the IEEE TRANSACTIONS ON ELECTRON DEVICES, the Past President of the IEEE Electron Devices Society, and a past elected member of the IEEE Board of Directors. In 2001, on behalf of the People to People Ambassadors Program, he led an Electron Devices Delegation to visit universities, government institutes, and companies in the People's Republic of China. He was the recipient of the 2004 IEEE Educational Activities Board Meritorious Achievement Award in Continuing Education "for extensive and innovative contributions to the continuing education of working professionals in the field of micro/nanoelectronics" and of the IEEE Electron Devices Society Distinguished Service Award in 2005. He currently holds the Bao Yugang Chair Professorship at Zhejiang University, Hangzhou, China.